DALTON
FULL PAPER

A comparative study of the synthesis, stereochemical characterization and reactivity of new chiral ruthenium(II) complexes with (aminoferrocenyl)phosphine ligands. X-Ray crystal structure of RuClH(cod)(PTFA) and Ru(η^3-C_8H_{13})Cl(PPFA) [PTFA = 1-diphenylphosphino-2,3-*endo*-(α-dimethylamino)tetramethyleneferrocene and PPFA = 2-(1-dimethylaminoethyl)-1-diphenylphosphinoferrocene] †

Félix A. Jalón,*[a] Ana López-Agenjo,[a] Blanca R. Manzano,[a] Montserrat Moreno-Lara,[a] Ana Rodríguez,[a] Thomas Sturm[b] and Walter Weissensteiner*[b]

[a] *Departamento de Química Inorgánica, Orgánica y Bioquímica, Facultad de Químicas, Campus Universitario, 13071 Ciudad Real, Spain. E-mail: fjalon@qino-cr.uclm.es*
[b] *Institut für Organische Chemie, Universität Wien, Währinger Straße 38, A-1090 Wien, Austria. E-mail: Walter.Weissensteiner@univie.ac.at*

Received 17th June 1999, Accepted 1st October 1999

The (aminoferrocenyl)phosphine ligands 2-(1-dimethylaminoethyl)-1-diphenylphosphinoferrocene (PPFA), 1-diphenylphosphino-2,1'-(1-dimethylaminopropanediyl)ferrocene (PAPF), and 1-diphenylphosphino-2,3-*endo*-(α-dimethylamino)tetramethyleneferrocene (PTFA) were used to synthesise new ruthenium(II) complexes. Reaction of RuClH(bpzm)(cod) [bpzm = bis(pyrazol-1-yl)methane, cod = 1,5-cyclooctadiene] with PTFA, PAPF or PPFA gave rise to the new hydride complexes: RuClH(cod)(NP), NP = PTFA, **1**; PAPF, **2**; PPFA, **3**. Complex **2** exists as two isomers with mutually *trans* hydride and chloride ligands that are oriented differently with respect to the aminophosphine ligand. It was not possible to isolate **3** in its pure form because it evolves in solution to Ru(η^3-C_8H_{13})Cl(PPFA) **4** as the final product. Reaction of $RuCl_2(PPh_3)_3$ with the (aminoferrocenyl)phosphine ligands gave $RuCl_2(PPh_3)$-(PTFA) **5** and the known complex $RuCl_2(PPh_3)$(PPFA). The reaction with PAPF led to a complex mixture. Complex **5** did not react with H_2 (5 atm) or superhydride but reaction with KBH_4 in EtOH gave rise to one or two isomers of the hydride RuH(η^2-BH_4)(PPh_3)(PTFA) **6**. The fluxional behaviour of the BH_4 group was studied and, for the major isomer, two different energy barriers were found for the hydride scrambling process. A two-step mechanism is proposed. The molecular structures of **1** and **4** were determined by X-ray diffraction.

Introduction

Ferrocenyl transition metal complexes have been studied extensively as enantioselective hydrogenation catalysts.[1] Quite recently, industrial applications of ferrocenyl rhodium and iridium complexes in the hydrogenation of imines and highly substituted alkenes have been announced.[2] In both cases, ferrocenyl diphosphine ligands related to PPFA (Chart 1) were used.

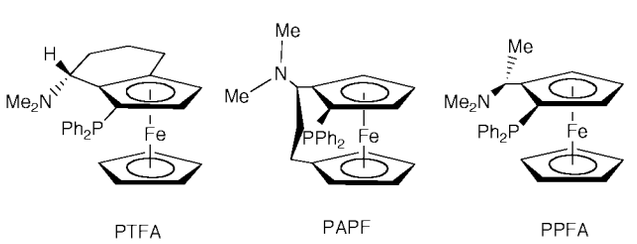

PTFA PAPF PPFA

Chart 1

In the study of hydrogenation catalysts, much less attention has been paid to the analogous ferrocenyl ruthenium complexes, although with Ru(PP) complexes (PP = binaphthyl or biphenyl based diphosphines) exceptional results could be obtained.[3] PPFA-type aminophosphines[4] and diphosphines[5] were investigated in hydrogenation reactions of terminal and internal alkenes. However, despite high chemical conversions, only low to moderate enantioselectivities were achieved.

For some time we have explored the structural and catalytic properties of transition metal complexes modified by ligands with either a homoannularly (PTFA) or heteroannularly (PAPF) (Chart 1) bridged ferrocenyl backbone including aminoalcohols, aminophosphines and diphosphines.[6] Both types of ligand are related to PPFA but are conformationally much less flexible, especially when coordinated to a transition metal complex.

In order to synthesise potential catalyst precursors for ruthenium-based hydrogenations using our aminophosphine ligands, synthetic routes to Ru hydride complexes of PTFA, PAPF and, for reasons of comparison, of PPFA were investigated. Structural as well as dynamic properties of these hydride complexes are discussed. It was found that the reactivities of these three ligands differ significantly from each other.

Results and discussion

Synthesis of the new complexes

When $RuCl_2$(bpzm)(cod) or RuClH(bpzm)(cod) [bpzm = bis-(pyrazol-1-yl)methane, cod = 1,5-cyclooctadiene], both of which were previously described by us,[7] were refluxed with

† *Supplementary data available*: rotatable 3-D crystal structure diagram in CHIME format. See http://www.rsc.org/suppdata/dt/1999/4031/

PTFA, PAPF, or PPFA, only the hydride complex reacted and this gave rise to new products [eqn. (1)].

$$RuClH(bpzm)(cod) + NP \longrightarrow RuClH(cod)(NP) + bpzm \quad (1)$$

NP	Complex
PTFA	**1**
PAPF	**2**
PPFA	**3**

The remaining bpzm was removed by chromatography on silica gel. Significant differences in reactivity were found depending on the aminophosphine ligand used. With PTFA only one isomer was obtained while two different isomers were formed with PAPF (a reaction time of four hours was used in both cases). Within the same period of time, the reaction with PPFA led to an evolution product, Ru(η^3-C_8H_{13})Cl(PPFA) **4**. With a shorter reaction time (one hour) the monohydride **3** was formed, although **4** was always present. Even at room temperature a transformation of **3** to **4** was observed, as demonstrated by ^{1}H-NMR spectroscopy (no intermediates were detected). Similar transformations have been previously described[8] for cationic ruthenium and iron derivatives of formula $[MH(cod)L_3]^+$, with L being different phosphines, phosphites or arsine ligands. The authors proposed that the hydride transfer depends essentially on the steric requirements of the ligands L. Complex **4** must be considered as the result of an insertion of one of the cyclooctadienyl alkene groups into the Ru–H bond of **3**, followed by successive addition–elimination reactions of β-hydrogens. The formation in these types of processes of an agostic transition state has been previously proposed in ruthenium chemistry and such a state is probably involved in the formation of **4**. In fact, in this complex a weak RuHC interaction has been observed (see below), which could be considered as the last step in this process.

When $RuCl_2(PPh_3)_3$ was used as the starting material, the reaction with PTFA in toluene led—after the displacement of two equivalents of PPh_3—to the formation of the new complex **5** [see eqn. (2)].

$$RuCl_2(PPh_3)_3 + PTFA \xrightarrow[-2PPh_3]{} \underset{\mathbf{5}}{RuCl_2(PPh_3)(PTFA)} \xrightarrow[-2KCl]{+\text{excess } KBH_4} \underset{\mathbf{6}}{RuH(\eta^2\text{-}BH_4)(PPh_3)(PTFA)} \quad (2)$$

The same reaction with PPFA gave rise to the previously described[4] $RuCl_2(PPh_3)$(PPFA), while reaction with PAPF led to a complex mixture.

Complex **5** did not react with H_2 (5 atm) or superhydride, but did react with KBH_4 in EtOH to yield the hydride complex **6**, which contains a bidentate BH_4 group. Depending on the reaction conditions employed, either one (r.t., 12 h) or two isomers (r.t., 2.5 h) were obtained. A similar reaction of $RuCl_2(PPh_3)$-(PPFA) with KBH_4 gave inseparable mixtures.

The new complexes are very soluble in common polar solvents and are also highly (**4**–**6**) or moderately (**1**–**3**) soluble in toluene or benzene. They are stable both in the solid state and in solution under an inert atmosphere. Complex **5** is air-stable in the solid state. The hydride derivatives reacted with halogenated solvents. In chloroform-*d*, **1** and **2** evolved to the dichloride complexes $RuCl_2$(cod)(NP), but it was not possible to isolate these new derivatives in their pure form. It should be mentioned that all of the new complexes described, including the borohydride complex **6**, can be expected to be potential precursors for hydrogenation reactions.[9]

Structural characterisation of the new complexes

Complexes RuClH(cod)(NP) (1, 2, 3). In solution only one isomer of **1** is observed, but two isomers of **2** (**2M** and **2m**) exist (M = major, m = minor). The ratio of **2M** to **2m** changes with the reaction conditions from 2:1 to 1.5:1. In the case of complex **3** only one isomer is seen in solution, although this is always observed along with its evolution product **4**. Hence, even in the first stages of the reaction the formation of a very reactive second isomer cannot be excluded. Considering the high steric requirements of cod and of the aminophosphine ligands, an arrangement of these two ligands in the equatorial plane of the octahedrally coordinated ruthenium is expected. In addition, the mutual *trans* position of hydride and chloride is favourable from an electronic point of view. Numerous examples of *trans*-positioned hydride and chloride substituents in the presence of a variety of other ligands have been described in the literature.[10] This *trans* arrangement has been confirmed to exist in complex **1** by an X-ray structure determination (see below).

In the infrared spectra an absorption band at 2015–2017 cm^{-1} confirms the existence of a terminal hydride in **1** and **2**. Some selected ^{1}H-, ^{13}C- and ^{31}P-{^{1}H}-NMR data are listed in Tables 1 and 2. The ^{1}H-NMR chemical shifts of the hydrides are in the range expected for *trans*-chloro-hydride Ru^{II} derivatives with coordinated cod[7,10a,b] and the HP-coupling constants are typical of a *cis* arrangement of phosphorus and hydride. It is interesting to note that, on considering the chemical shifts of hydride and phosphorus as well as the coupling constants J_{HP}, a classification of these four complexes into two groups can be made: **1** and **2M** on the one hand (δ_H = −6.21, −6.60; δ_P = 38.58, 39.14; J_{HP} = 18.5, 18.0 Hz, respectively) and, on the other hand, **3** and **2m** (δ_H = −7.86, −8.24; δ_P = 20.13, 23.80; J_{HP} = 26.6, 27.8 Hz, respectively). This pattern is likely to be characteristic for the two types of diastereomers with the hydride either in an *endo* or in an *exo* arrangement (hydride toward or away from the ferrocenyl core, respectively; see Chart 2).

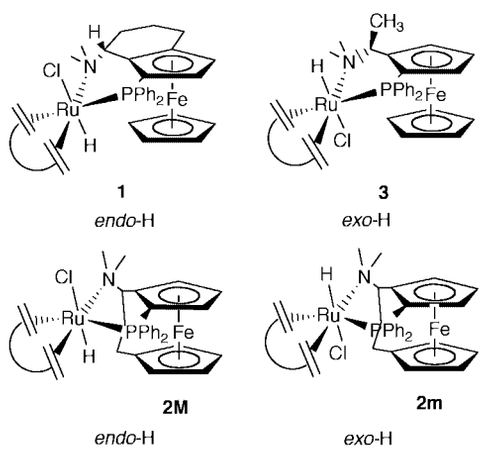

Chart 2 Proposed structures for the RuClH(cod)(NP) complexes **1**–**3**.

Taking into account that an *endo* structure has been found for **1** (see below for discussion of the X-ray data), an *endo* configuration is also assigned to **2M**, whereas in **3** and **2m** the hydride adopts an *exo* position. The observation of NOEs between the hydrides of complexes **1** and **3** and the nearest aminomethyl groups, situated either below (**1**) or above (**3**) the functionalised Cp ring, confirms this assignment.

The NMR spectra of **1**–**3** show the expected characteristics of a bidentate N,P coordination of the aminophosphine ligands: for example, the appearance of two diastereotopic aminomethyl groups in both ^{1}H- and ^{13}C-NMR spectra (N-coordination) and a deshielding of the phosphorus resonances with respect to the free ligands.[11] The two very different coup-

Table 1 Selected ^{1}H-NMR data for ligands and complexes **1**–**6**[a]

Compound	Cp^2	Cp^1	$N(CH_3)_2$	H_α	Ru–H
PTFA	3.97 (s)	3.95 (d) J_{HH} = 2.2 3.37 (s)	2.27 (s)	2.9 (m)	
PAPF	3.71 (s, 2H) 3.86 (s) 4.08 (s) 4.15 (s) 4.18 (s) 4.39 (s)		1.82 (s)	2.62 (dd) J_{HH} = 15; J_{HH} = 3.6	
PPFA	3.94 (s)	4.35 (s) 4.23 (s) 3.82 (s)	1.76 (s)	4.15 (m)	
1	3.52 (s)	4.20 (t) J_{HP} = 2.4 4.40 (d) J_{HH} = 2.4	2.25 (s) 3.30 (s)	4.70 (dd) J_{HH} = 11; J_{HH} = 2.9	−6.21 (d) J_{HP} = 18.5
2M	3.60 (s) 3.65 (s) 3.81 (s) 4.11 (s) 4.29 (s) 4.42 (s)		2.32 (s) 2.40 (s)	[b]	−6.60 (d) J_{HP} = 18.0
2m	3.62 (s) 3.81 (s) 4.07 (s) 4.24 (s) 4.41 (2H)		2.51 (s) 2.91 (s)	[b]	−8.24 (d) J_{HP} = 27.8
3	3.76 (s)	4.06 (bs) 3.69 (bs) 3.94 (bs)	3.6 (s) 2.2 (bs)	6.06 (q) J_{HH} = 6.8	−7.86 (d) J_{HP} = 26.6
4	3.76 (s)	4.13 (bs) 3.89 (t) J_{HH} = 2.4 3.81 (bs)	2.93 (s) 3.56 (s)	6.70 (q) J_{HH} = 6.8	
5	3.48 (s)	4.13 (t) J_{HP} = 2.4 4.29 (d) J_{HH} = 2.4	2.81 (d) J_{HP} = 1.5 3.63 (d) J_{HP} = 1.7	5.19 (dd) J_{HH} = 10.8; J_{HH} = 3.7	
6M	3.20 (s)	3.81 (bs) 3.96 (bs)	3.08 (s, U) 3.34 (s, D)	4.61 (d) J_{HH} = 11.5	−13.29 (t) J_{HPa} = J_{HPb} = 30.3
6m	3.52 (s)	4.18 (d) J_{HP} = 2.4 4.06 (t) J_{HH} = 2.4	3.08 (s) 3.34 (s)	[b]	−14.39 (dd) J_{HPa} = 24.3 J_{HPb} = 34.9

[a] Recorded at room temperature in benzene-d_6 (PTFA, **3** and **4**), toluene-d_8 (**6**), acetone-d_6 (**1**, **2**) or chloroform-*d* (PAPF, PPFA, **5**). M = major isomer; m = minor isomer; s = singlet; bs = broad singlet; d = doublet; t = triplet; q = quartet; m = multiplet; D = down, U = up. Coupling constants (Hz) are listed with the corresponding resonance. Phenyl protons are in the range 9.2–6.8 ppm. Alkylic protons for the cod ligand and the homo- (PTFA) or hetero-annular (PAPF) chains are in the range of 1.2–3.0 ppm. Cp^1 refers to the P-functionalized cyclopentadienyl group. For the adopted numbering scheme see Charts 2–4. For **6**, P_a refers to PPh_3 and P_b to PTFA. For additional information see Experimental section. [b] Non-identified signals.

Table 2 Selected ^{13}C and ^{31}P-{^{1}H}-NMR data for complexes **1**–**6**[a]

Compound	Cp^2	Cp^1	$N(CH_3)_2$	C_α	^{31}P
1	72.46 (s)	89.1 (d), J_{CP} = 17.5 86.47 (d), J_{CP} = 9.01 71.39 (s) 69.67 (d), J_{CP} = 4.0 68.16 (s)	48.20 (s) 41.07 (s)	61.24 (s)	38.58 (s)
2M		[b]	58.10 (s) 60.60 (s)	67.93 (s)	39.14 (s)
2m		[b]	53.53 (s) 56.18 (s)	64.94 (s)	23.80 (s)
3	—	—	—	—	20.13 (s)
4	71.11 (s)	95.02 (d), J_{CP} = 18 69.44 (d), J_{CP} = 8.6 69.04 (d), J_{CP} = 6.9 72.63 (s)	47.13 (s) 49.39 (s)	57.77 (s)	88.85 (s)
5	71.83 (s)	96.32 (d), J_{CP} = 17.2 85.18 (d), J_{CP} = 8.0 73.24 (d), J_{CP} = 50.8 69.37 (s) 68.24 (d), J_{CP} = 5.6	44.55 (d), J_{CP} = 2.6 42.27 (d), J_{CP} = 1.3	60.28 (s)	73.12 (d), J_{PP} = 36.6, PTFA 39.30 (d), PPh_3
6M	71.97 (s)	96.63 (d), J_{CP} = 18.1 84.71 (d), J_{CP} = 7.6 77.35 (d), J_{CP} = 37.3 71.32 (s) 67.25 (d), J_{CP} = 4.5	55.23 (s) 55.09 (s)	64.37 (s)	70.12 (d), J_{PP} = 29.9, PPh_3 68.53 (d), PTFA
6m	71.93 (s)	[c]	[c]	[c]	71.74 (d), J_{PP} = 34.8, PPh_3 59.21 (d), PTFA

[a] Recorded at room temperature in benzene-d_6 (**2**–**4** and **6**), acetone-d_6 (**1**) or chloroform-*d* (**5**). M = major isomer; m = minor isomer. Coupling constants (Hz) are listed with the corresponding resonance. Phenyl carbons are in the range 124–126 ppm. Cp^1 refers to the P-functionalized cyclopentadienyl group. For additional information see Experimental section. [b] Cp^1 and Cp^2 signals could not be unequivocally assigned to the major and minor isomer, respectively. [c] Signals not clearly observed.

ling constants observed for the H_α (see Chart 3) resonance of **1** ($^3J_{HH}$ = 11, 2.9 Hz) imply a strongly preferred rigid pseudo-equatorial arrangement of the dimethylamino group in the six-membered ring (Conformation A in Chart 3).

In complexes with PAPF, the possibility of conformational isomers can be ruled out. Although in principle two conformations[6d] are possible for non-coordinated PAPF (see Chart 4), only conformation (a), which according to previous calculations[6d] is 22 kJ mol^{-1} more stable than conformation (b), is suitable for chelate coordination. In this orientation the hetero-

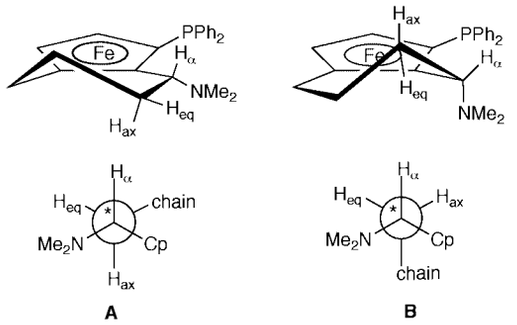

Chart 3 The two possible conformations of the six-membered ring in PTFA ligand.

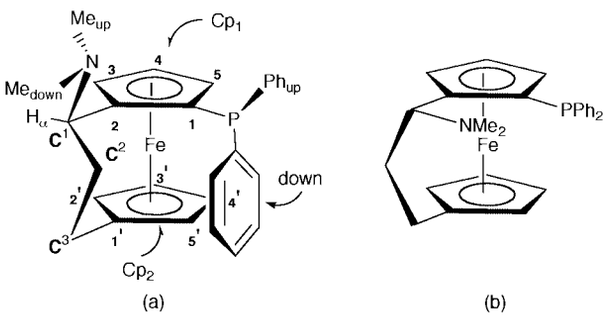

Chart 4 Preferred (a) and less stable (b) conformation of ligand PAPF. Numbering scheme of PAPF (a).

annular chain has the central carbon pointing towards the phosphorus atom and, as a consequence, the NMe_2 group is located above the Cp^1 plane.

Molecular structure of 1. The molecular structure of complex **1** was solved by an X-ray diffraction analysis. Racemic complex **1** crystallises in the monoclinic space group $P2_1/n$ with four molecules in the unit cell. The corresponding ORTEP representation is shown in Fig. 1.

Crystallographic data are summarised in Table 3 and selected bond lengths and bond angles are given in Table 4. The ruthenium atom has a distorted octahedral environment. The chloride and the hydride are in apical positions with the hydrogen atom directed toward the ferrocene unit (*endo* isomer). The distortion essentially affects the bond angles Cl3–Ru–Ctr(1) and Cl3–Ru–Ctr(2) [100.54(2) and 102.42(2)°, respectively] where Ctr(1) = centroid of the C(34)–C(41) bond, Ctr(2) that of C(37)–C(38). As a consequence, the bond angle Cl3–Ru–H1 is reduced to 166.72(97)°. This type of distortion has already been observed in similar complexes of formula $RuClH(cod)L_2$ (L = pyridine or piperidine)[10a,b] and also in other *trans*-chlorohydride ruthenium complexes[10c–e] with different ancillary ligands.

In the PTFA ligand the dimethylamino group adopts a pseudo-equatorial conformation with the nitrogen 0.123(2) Å below Cp^1. In the six-membered ring C9 is located on the proximal and C10 on the distal side of the functionalised Cp group [C9, 0.286(3) below and C10, 0.4233(3) Å above the plane]. In this particular conformation the ruthenium centre is positioned above Cp^1 [0.8778(3) Å] and H8 is in a pseudo-axial position pointing toward the chloride ligand.

In the chelate ring formed by ruthenium and the ferrocenyl ligand, one phenyl and one methyl group are each located in a pseudo-axial position and are pointing toward the ferrocenyl core. These groups, together with two CH= moieties of the cod ligand, form a hydrophobic pocket around the hydride. This preferred location in hydrophobic pockets has been previously observed in Ir^{III} hydride derivatives with diphosphine ferrocenyl ligands.[12] In addition, the overall structural features clearly indicate that the arrangement of the chloride in an *exo* position

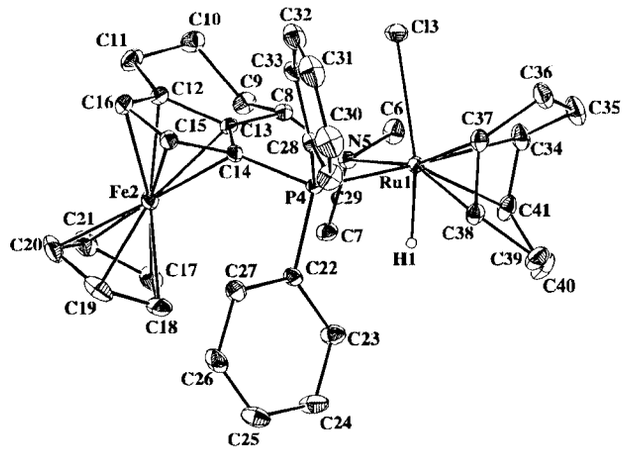

Fig. 1 ORTEP drawing of the molecular structure of RuClH(cod)-(PTFA), **1**.

is sterically less demanding than in an *endo* position since an *endo* chloride is expected to strongly interact with proton H7 in particular, but also with protons H38 and H41. A similar situation is also expected for a complex with the NMe_2 group in a pseudo-axial position, such as that found in the $(PTFA)PdCl_2$ complex.[6a] Hence, we assume that steric interactions and the hydrophobic character of the pocket formed in this particular conformation of the ferrocenyl ligand prevent the formation of the second isomer of **1** with the hydride located in an *exo* position.

Complex 5. The ^1H-, ^{13}C- and ^{31}P-$\{^1H\}$-NMR of **4** exhibit the expected resonances for the coordinated PPFA ligand. The anomalously low field chemical shift (88.85 ppm) of the ^{31}P-NMR resonance (as compared to **3** or palladium complexes) is worthy of note.[11] This must be due to the special position of the phosphorus atom in this molecule with a vacant coordination site in a *trans* position (see Fig. 2 for the X-ray structure).

The assignment of the cyclooctenyl ^1H-NMR resonances is based on a ^1H–^1H COSY experiment and was confirmed by NOE studies. The ^{13}C-NMR signals were assigned by a heteronuclear ^1H–^{13}C COSY experiment. The asymmetric environment of this ligand is confirmed by the appearance of thirteen ^1H-NMR and eight ^{13}C-NMR resonances. More importantly, the signal of the *endo* proton H8B is found at −0.55 ppm while the analogous *endo* hydrogen H4A resonates at 0.65 ppm. In the complexes[8] $[M(\eta^3\text{-}C_8H_{13})L_3]^+$ (M = Ru, Fe) described above this type of shielding is even more pronounced (−1.4 to −2.4 ppm). In these cationic complexes an agostic interaction with the *endo* protons has been established. Although the C8 is not especially shielded in the ^{13}C-NMR spectrum of **4**, this is the only carbon to show a coupling (4.5 Hz) with phosphorus. In addition, the $^1J_{C\text{-}H}$ observed for this carbon is smaller (105 Hz) than those of the rest of the C–H groups in this ligand (*ca.* 120 Hz). All these data indicate a remote[13,14] interaction in solution. In order to obtain additional evidence of such an interaction, we decided to perform an X-ray diffraction study on **4**.

Molecular structure of 4. Racemic complex **4** crystallises in the monoclinic space group $P2_1/c$ with four molecules in the unit cell. Two orientations of the corresponding molecular structure are depicted in Fig. 2 and 3. Crystallographic data are summarised in Table 3 and a selection of bond lengths and bond angles can be found in Table 4. The coordination geometry around the ruthenium centre is irregular square pyramidal with P4 occupying the axial site, Cl3 and N5 situated in basal sites *cis* to each other, and the η^3-enyl fragment of the cyclooctenyl ligand coordinated across the two remaining basal sites. The Ru–P4 bond distance of 2.1666(7) Å is within the typical range[15,8d] of axial Ru–P bond lengths in 16 electron square pyramidal complexes. This value is clearly shorter than

Table 3 Crystal data and structure refinement for **1** and **4**

	1	**4**
Chemical formula	$C_{36}H_{43}ClFeNPRu$	$C_{34}H_{41}ClFeNPRu$
Formula weight	713.05	687.02
T/K	293(2)	293(2)
Crystal system	Monoclinic	Monoclinic
Space group	$P2_1/n$	$P2_1/c$
a/Å	11.2600(10)	9.477(5)
b/Å	22.998(8)	16.1020(10)
c/Å	12.0024(9)	20.281(3)
β/°	91.369(7)	103.57(2)
V/Å^3	3107.2(11)	3009(2)
Z	4	4
Absorption coefficient/cm^{-1}	11.17	11.51
Transmission range	0.998–1.000	0.830–1.000
Reflections collected	14767	7239
Independent reflections	7474 [*R*(int) = 0.0196]	7239 [*R*(int) = 0.0000]
Final *R* indices [$I > 2\sigma(I)$]	$R_1 = 0.0260$, $wR_2 = 0.0608$	$R_1 = 0.0248$, $wR_2 = 0.0615$
R indices (all data)	$R_1 = 0.0425$, $wR_2 = 0.0807$	$R_1 = 0.0432$, $wR_2 = 0.0835$

Table 4 Bond lengths (Å) and angles (°) for **1** and **4**

1			
Ru(1)–H(1)	1.51(2)	C(41)–Ru(1)–P(4)	147.99(9)
Ru(1)–C(34)	2.252(3)	C(37)–Ru(1)–P(4)	93.93(8)
Ru(1)–C(37)	2.163(3)	C(38)–Ru(1)–P(4)	87.83(8)
Ru(1)–C(38)	2.171(3)	C(34)–Ru(1)–P(4)	172.38(9)
Ru(1)–C(41)	2.221(3)	C(37)–Ru(1)–N(5)	165.65(9)
Ru(1)–P(4)	2.3118(8)	C(38)–Ru(1)–N(5)	156.25(9)
Ru(1)–N(5)	2.365(2)	C(41)–Ru(1)–N(5)	90.66(10)
Ru(1)–Cl(3)	2.5281(8)	C(34)–Ru(1)–N(5)	96.70(9)
C(34)–C(41)	1.380(5)	P(4)–Ru(1)–N(5)	90.06(5)
C(34)–C(35)	1.517(5)	C(37)–Ru(1)–Cl(3)	81.70(8)
C(35)–C(36)	1.511(5)	C(38)–Ru(1)–Cl(3)	119.84(9)
C(36)–C(37)	1.500(4)	C(41)–Ru(1)–Cl(3)	119.84(9)
C(37)–C(38)	1.409(4)	C(34)–Ru(1)–Cl(3)	85.13(9)
C(38)–C(39)	1.522(4)	N(5)–Ru(1)–Cl(3)	84.39(5)
C(39)–C(40)	1.504(5)	P(4)–Ru(1)–Cl(3)	92.07(3)
C(40)–C(41)	1.519(4)		
4			
Ru(1)–C(1)	2.142(3)	P(4)–Ru(1)–N(5)	93.74(5)
Ru(1)–C(2)	2.095(3)	C(3)–Ru(1)–C(1)	71.04(11)
Ru(1)–C(3)	2.151(3)	C(2)–Ru(1)–N(5)	136.77(10)
Ru(1)–P(4)	2.1666(7)	C(2)–Ru(1)–Cl(3)	133.51(9)
Ru(1)–N(5)	2.295(2)	P(4)–Ru(1)–Cl(3)	103.19(4)
Ru(1)–Cl(3)	2.4611(13)	N(5)–Ru(1)–Cl(3)	87.60(6)
C(1)–C(2)	1.412(4)	C(2)–C(1)–C(8)	123.3(3)
C(1)–C(8)	1.503(4)	C(1)–C(2)–C(3)	123.2(3)
C(2)–C(3)	1.424(4)	C(2)–C(3)–C(4)	124.2(3)
C(3)–C(4)	1.519(4)	C(3)–C(4)–C(5)	115.2(3)
C(4)–C(5)	1.542(5)	C(6)–C(5)–C(4)	116.6(3)
C(5)–C(6)	1.512(5)	C(7)–C(6)–C(5)	118.0(3)
C(6)–C(7)	1.507(5)	C(6)–C(7)–C(8)	116.7(3)
C(7)–C(8)	1.560(5)	C(1)–C(8)–C(7)	116.2(3)

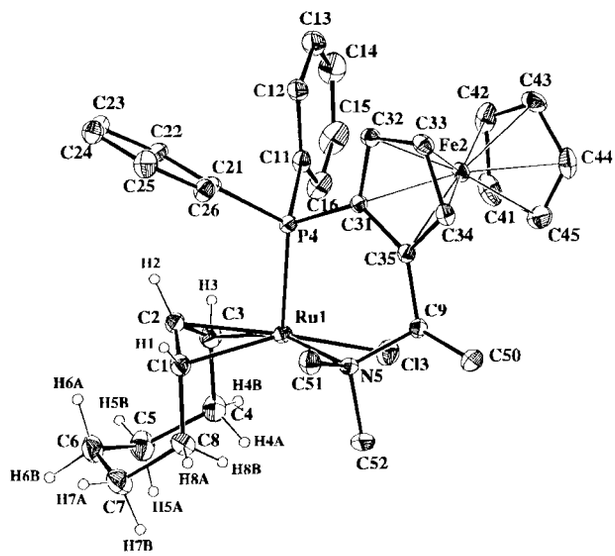

Fig. 2 ORTEP drawing of the molecular structure of $RuCl(\eta^3\text{-}C_8H_{13})(PPFA)$, **4**.

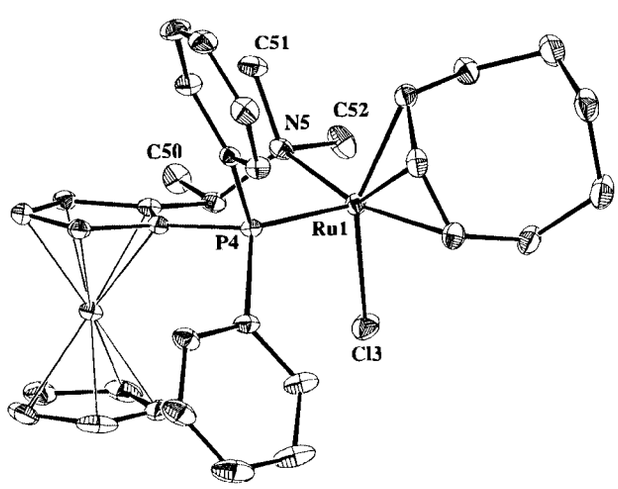

Fig. 3 ORTEP drawing of the molecular structure of complex **4** especially focusing on the conformation of the ferrocenyl ligand.

that found in the octahedral complex **1** [2.3118(8) Å], which justifies the strong low field shift of the ^{31}P-NMR resonance in **4**. The bite angle of the PPFA ligand (P4–Ru1–N5) is 93.74(5)°.

The η^3-cyclooctenyl ligand adopts a boat conformation with the alkyl moiety below the basal plane of the molecule. A selection of bond distances characteristic for the coordinated cyclooctenyl ligand is given in Chart 5(c) along with data for the analogous iron, (a), and ruthenium, (b), complexes.[8] The Ru–$C_{allylic}$ bond distances in **4** are shorter than those in the respective complex listed in Chart 5(b) and are also shorter than those of other enyl-ruthenium derivatives[16] indicating a stronger interaction with the metallic centre in complex **4**. In (a), a strong agostic interaction C8–H8$_{endo}$ $\cdots$ M has been found. This type of interaction, although weaker, has also been proposed for structure (b). This situation was mainly deduced from the short Ru–H8 and Ru–C8 bond distances (the numbering scheme shown in Chart 5 is used). In complex **4** the distance Ru–H8B (*endo*) [2.671(3) Å] is shorter than the sum of the Van der Waals radii and also shorter than the corresponding Ru–H4A(*endo*) distance [2.82(3) Å]. This Ru–H8B distance falls in the range of weak agostic interactions observed for organometallic compounds of the "platinum" metals.[13a]

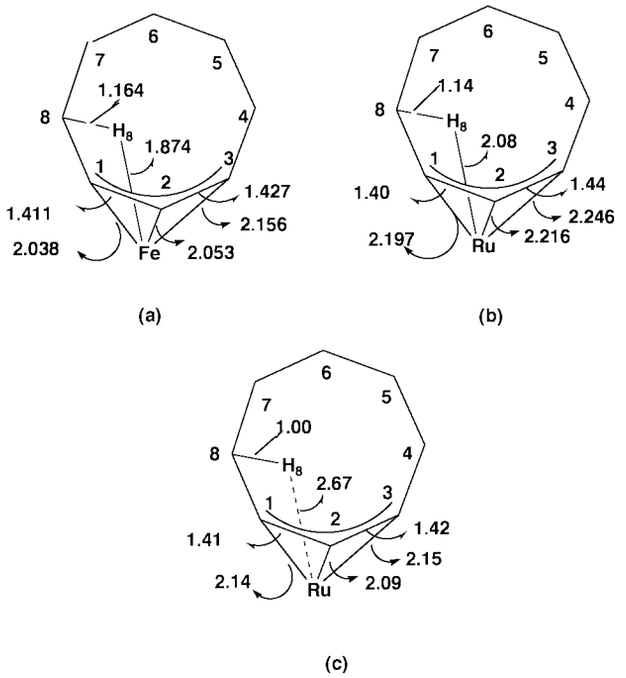

Chart 5

This distance, along with the previously described spectroscopic characteristics of complex **4**, points to the existence of a weak agostic C8–H8B · · · Ru interaction for **4** both in solution and in the solid state.

The conformation of the chelate ring shown in Fig. 3 is similar to those found in many other PPFA complexes. The ruthenium atom and the NMe_2 group are located above the functionalised Cp^1 plane [0.4167(4) and 0.96(2) Å, respectively] with C(50) in a pseudo-equatorial position slightly below the Cp^1 plane [0.015(3) Å].

Complexes $RuCl_2(PPh_3)$(PTFA) 5 and $RuH(\eta^2\text{-}BH_4)(PPh_3)$-(PTFA) 6. The IR spectrum of complex **5** shows a single absorption band at 322 cm^{-1}, which is characteristic of ν(Ru–Cl) with mutual *trans*-chlorides.[4,17]

In the $^{31}P\{^1H\}$-NMR spectrum of **5** (see Table 2) two doublets are observed with a coupling constant (J_{PP} = 36.6 Hz) typical of a *cis* arrangement. The resonance at low field (73.12 ppm) is assigned to the PTFA phosphorus by selective irradiation, which causes the disappearance of the characteristic H–P coupling constant of the *ortho* hydrogens of the PTFA phenyl groups. As discussed above for complex **4**, the low field chemical shift of this resonance is thought to be indicative of a position of this atom *trans* to a vacant coordination site.

As in **1**, the doublet of doublets due to the H_a resonance of **5** is indicative of a pseudo-equatorial position of the dimethylamino group in the six-membered ring.

All the spectral data for complex **5** are consistent with a square pyramidal environment of the ruthenium centre, as depicted schematically in Chart 6. Such a structure has been

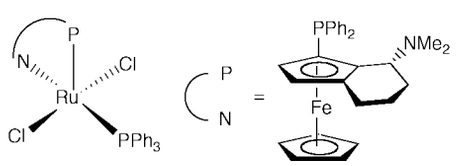

Chart 6 Proposed schematic structure for **5**.

found for a similar complex, $RuCl_2(PPh_3)$(*iso*-PFA) [*iso*-PFA = $(\eta^5\text{-}C_5H_5)Fe(\eta^5\text{-}C_5H_3(CHMeNMe_2)P(i\text{-}Pr_2\text{-}1,2)]$, in the solid state.[15a]

As stated above, two isomers of **6**, *i.e.* **6M** and **6m**, can be

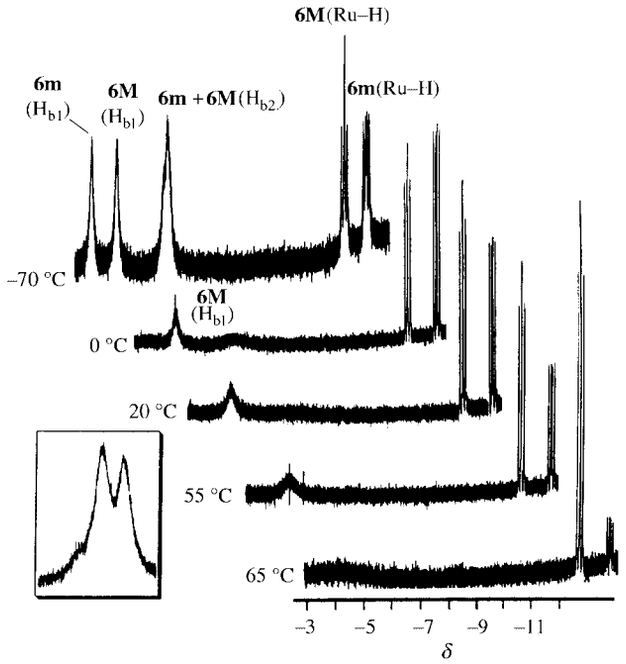

Fig. 4 Hydride region of the variable temperature ^{1}H-NMR spectra of complex **6**. The inset corresponds to the appearance of the H_{b2} (**6M** + **6m**) signal in a sample where **6m** was present in a small ratio. The doublet of **6M** is clearly observed. The assignment has been confirmed by selective ^{31}P decoupling.

obtained with an isomer ratio that is strongly dependent on the experimental conditions, with one particular isomer always being the major component of the mixture. At temperatures above 50 °C the irreversible transformation of **6m** into the thermodynamically more stable isomer **6M** takes place.

The IR spectrum of **6** shows a ν(Ru–H) band at 2042 cm^{-1}, which is characteristic of a terminal hydride. The BH_4 group attached to the Ru centre shows characteristic bands that support the existence of both terminal [$\nu(B\text{–}H_t)$ = 2371 and 2300 cm^{-1}] and bridging [$\nu(Ru\text{–}H_b\text{–}B)$ = 1914 and 1900 cm^{-1}] hydrides, in a similar way to previously reported covalent Ru-BH_4 complexes.[18,19] In the $^{31}P\{^1H\}$-NMR of **6** two doublets are observed for each isomer, with coupling constants typical of a mutual *cis* orientation of the phosphorus atoms. No additional information could be obtained from the ^{11}B-NMR spectrum, which shows two very broad signals over the whole temperature range studied (−40 to 60 °C).

The hydride region of the ^{1}H-NMR spectrum at room temperature shows two signals for the terminal hydrides with different integrals corresponding to different isomers: a pseudo-triplet (−13.29 ppm, **6M**) and a doublet of doublets (−14.39 ppm, **6m**) with coupling constants typical of a *cis* orientation with respect to the two different phosphorus nuclei. This has been confirmed by selective irradiations of the corresponding $^{31}P\text{-}\{^1H\}$-NMR signals. In addition, a very broad signal is observed at about −5 ppm that corresponds to the bridging hydrogens of a BH_4 group coordinated to the ruthenium centre (see Fig. 4). This broad signal and the absence of resonances of the terminal BH_t groups seems indicative of a fluxional behaviour, and so the spectra were also recorded at low temperature in order to identify the signals separately and to establish the coordination mode of the BH_4 group. At −70 °C, four new resonances (two for each isomer: one broad singlet and one broad doublet with identical integrals) appear in place of the broad signal in the chemical shift region typical of $Ru\text{–}H_b\text{–}B$ groups. The doublets show a coupling constant indicative of a *trans* coordinated phosphorus nucleus.

This nucleus has been identified by selective irradiation as the PTFA phosphorus. Two additional broad resonances are seen at lower field with identical integrals and these are assigned to

the B–H_t signals of **6M**. The corresponding B–H_t resonances of **6m** are hidden due to overlap with signals of other groups. All these data indicate that the BH_4 group in both isomers is coordinated in a bidentate fashion within very similar asymmetric chemical environments. Both structures differ only in the apical position to which the BH_4 group is bound. A low temperature NOE study allowed the unequivocal assignment of the structure of **6M** as that shown in Chart 7. Irradiation of the

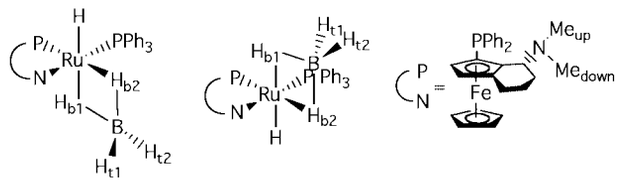

Chart 7 Proposed schematic structures for the isomers of complex **6**.

terminal hydride resulted in NOEs in both the *ortho* phenyl hydrogens of the Ph_{down} and in the NMe_{down} signals. The down orientation (*i.e.* towards the ferrocenyl core) of these two groups is deduced from its NOE with the unfunctionalised Cp ring.

According to the ^{1}H- and ^{13}C-NMR data the conformation of the six-membered chelate ring of the PTFA ligand is similar to those found in complexes **1** and **5**.

Fluxional behaviour of the BH_4 group in 6. A selection of the ^{1}H-NMR spectra of **6** recorded at different temperatures (−70 to 65 °C) in toluene-d_8 is shown in Fig. 4. At low temperature almost all resonances of the boron-hydrogen atoms are seen independently for both isomers. As the temperature is increased to 20 °C all these signals broaden and finally disappear into the baseline, apart from the resonance assigned to the hydride BH_{b1} of **6M**. It was not possible to observe the narrowing signals at higher temperature, which is most likely due to the high chemical shift difference (*ca.* 2400 Hz). When the temperature was increased the BH_{b1} resonance broadened even when the spectrum was boron (^{11}B) decoupled and at 65 °C the signal finally collapsed. The practically unchanged chemical shift of this last resonance, at around −4.4 ppm, suggests that H_{b1} remains in an identical environment *trans* to the terminal Ru–H hydride during the fluxional process that exchanges the other three hydrogen atoms of the BH_4 group. On the other hand, the terminal Ru–H resonances of both isomers remain sharp throughout the studied temperature range, indicating that these hydrides do not participate in the fluxional process of the BH_4 ligand.

The VT-NMR data for both isomers of **6** are in agreement with a two step process (Scheme 1) that can explain the observed scrambling of the bridging and of the terminal hydrogen atoms in the BH_4 units. In a first step, an η^2-η^1 transformation takes place (Scheme 1, path a). In a theoretical study of such a scrambling process in osmium complexes, this type of η^1 intermediate has been proposed as the most favourable one.[20] This Ru–H_{b2} bond opening is followed by a rotation around the B–H_{b1} bond (Scheme 1, path b), which allows the interconversion of the other three hydrogens of the BH_4 group. The scrambling of the fourth hydride, H_{b1}, could take place *via* the alternatives (path c1) or (path c2). In the stepwise process (path c1) a reorganisation of the unsaturated intermediate occurs in such a way that, initially, H_{b1} is positioned *trans* to the ferrocenyl phosphorus. In such a situation, any of the other three hydrogens can occupy the vacant site *trans* to the Ru–H ligand. Alternatively, H_{b1} could interchange with the other three hydrogens, either by a complete dissociation of the BH_4 group to give an ionic pair, $[RuH(PPh_3)(PTFA)]^+[BH_4]^-$, or *via* a concerted mechanism (path c2). In these cases a reorganisation of the intermediate geometry does not take place. For isomer **6m** a

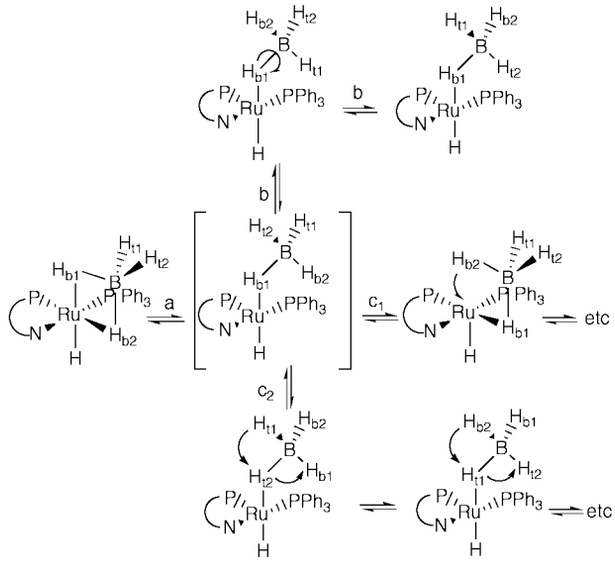

Scheme 1 Proposed mechanism for the fluxional behaviour of both isomers of **6**. (a) Ru–H_{b2} bond rupture; (b) rotation of the BH_3 unit around B–H_{b1}; (c) exchange of H_{b1} *via* a stepwise (c_1) or a concerted (c_2) process.

simultaneous coalescence of the four signals has been observed; hence, these two consecutive steps must have comparable energy barriers. However, in **6M** it is clear that step (a) must be of lower energy than step (c). Meek *et al.*[19] have studied the fluxional behaviour of a BH_4 group in the complex RuH(BH_4)(ttp) [ttp = $PhP(CH_2CH_2CH_2PPh_2)_2$] and have also found a two step interchange mechanism. However, two main differences are worth noting: (i) the energy difference between the two steps is higher for complex **6M**, which shows an especially low barrier for the formation step of the η^1-intermediate and (ii) this intermediate is formed selectively with the H_{b1} situated *trans* to the hydride instead of being *trans* to phosphorus, as occurs in the RuH(BH_4)(ttp) complex. The behaviour of complex **6M** is not in accordance with the higher *trans* influence of the hydride as compared to tertiary phosphines. This fact is not yet well understood, but the special stability of square pyramidal geometries with the phosphorus atom in the apical position, like in ferrocenyl aminophosphine derivative **4**, might be the origin of this behaviour. The relative stability of this intermediate is also in accordance with the lower energy barrier observed for the first step in **6**. A comparison of structures **6m** and **6M** (Chart 7) shows that in both cases the Ru–H_{b2} bond breaking process leads to a pentacoordinated intermediate but that the intermediate formed from **6m** will suffer from a higher steric interaction between the *endo*-BH_4 group and the space-demanding ferrocenyl core. As a consequence, this intermediate is expected to be thermodynamically less stable.

Conclusions

New chloro-hydride ruthenium complexes containing (aminoferrocenyl)phosphine ligands of formula RuClH(cod)(NP) **1**–**3** have been prepared. A high selectivity has been observed in the formation of these complexes with the chloro and hydride groups always occupying a mutual *trans* position. Only in the case of PAPF have two isomers been observed. The molecular structure of complex **1** was determined by an X-ray diffraction study. The complex RuClH(cod)(PPFA) evolves spontaneously towards the formation of the cyclooctenyl complex Ru(η^3-C_8H_{13})Cl(PPFA) **4**. For this complex a weak agostic interaction has been proposed to exist both in solution and in the solid state (X-ray structure analysis), which is in contrast to other known isoelectronic derivatives. The unsaturated square pyramidal complex $RuCl_2(PPh_3)$(PTFA) **5** has also been synthesised. This compound reacts with KBH_4 to give the derivative

$RuH(\eta^2\text{-}BH_4)(PPh_3)$(PTFA) **6**, which, depending on the reaction conditions, is isolated in its pure form or as a mixture of two isomers. The scrambling of the BH_4 hydrides has also been studied. A stereoselective two-step mechanism involving η^1 intermediates with different barriers for the two isomers has been proposed. From the results obtained it can be concluded that the nature of the ligand clearly affects both the stereochemistry and the reactivity of these new complexes. Assessment of the catalytic properties of these complexes will be performed in due course.

Experimental

General comments

All manipulations were carried out under an atmosphere of dry oxygen-free nitrogen using standard Schlenk techniques. Solvents were distilled from the appropriate drying agents and degassed before use. Elemental analyses were performed with a Perkin-Elmer 2400 microanalyser. IR spectra were recorded as KBr pellets or Nujol mulls with a Perkin-Elmer PE 883 IR spectrometer. ^{1}H, ^{13}C and ^{31}P-{^{1}H}-NMR spectra were recorded on a Varian Unity 300 spectrometer. Chemical shifts (ppm) are relative to TMS (^{1}H-, ^{13}C-NMR), and 85% H_3PO_4 (^{31}P-NMR). Coupling constants (*J*) are in Hertz. The NOE difference spectra were recorded with 5000 Hz, acquisition time 3.27 s, pulse width 90°, relaxation delay 4 s, irradiation power 5–10 dB, number of scans 240. For variable temperature spectra, the probe temperature (±1 K) was controlled by a standard unit calibrated with a methanol reference. RuClH(bpzm)(cod),[7] $RuCl_2(PPh_3)_3$ [21] and ligands PTFA,[6a] PAPF [6d] and PPFA [22] were prepared according to literature methods. KBH_4 was purchased from Aldrich-Chimica.

Preparation of RuClH(cod)(PTFA) 1. To a degassed suspension of RuClH(bpzm)(cod) (66 mg, 0.17 mmol) in 10 mL of THF, 80 mg (0.17 mmol) of PTFA were added. The mixture was refluxed for 4 h and evaporated to dryness. Chromatography on Silica 60 (25 × 1 cm) using THF–Et_2O = 9 : 1 as eluent allowed the separation of free bpzm and complex **1**. The orange band containing complex **1** was recovered in a Schlenk tube and the solvent evaporated to dryness. Crystals of pure **1** were obtained by vapour diffusion from THF–pentane. Yield: (85.5 mg, 70%). Found: C, 60.5; H, 5.7 ; N, 2.1. $C_{36}H_{43}$ClNPFeRu requires C, 60.7; H, 6.0; N, 2.0%. IR: ν_{max}/cm^{-1} 2017 (Ru–H) and 277 (Ru–Cl). ^{1}H-NMR (acetone-d_6): δ 3.92 (2H, m, H_{olef}^{cod}); 4.57 (2H, m, H_{olef}^{cod}). ^{13}C{^{1}H}-NMR (acetone-d_6): δ 24.75, 24.0, 20.82 (s, homoannular chain); C_{olef}^{cod}: 71.80 (2C, s); 64.89 (s); 63.03 (s); C_{alk}^{cod}: 36.68 (d, J_{CP} = 3.0); 28.28 (d, J_{CP} = 3.0); 24.84 (s); 24.67 (s).

Preparation of RuClH(cod)(PAPF) 2. The procedure is identical to that described for **1**. Amounts are as follows: RuClH(bpzm)(cod): 70.9 mg, 0.18 mmol; PAPF: 81.5 mg, 0.18 mmol. Complex **2** was obtained as an orange solid (**2M** = 55%; **2m** = 45%). Yield: (40.25 mg, 32%). Found: C, 59.9; H, 5.9 ; N, 2.0. $C_{35}H_{41}$ClNPFeRu requires C, 60.1; H, 5.9; N, 2.0%. IR: ν_{max}/cm^{-1} 2015 (Ru–H) and 253 (Ru–Cl). **2M** or **2m**: ^{1}H-NMR (acetone-d_6): δ 4.61 (m, H_{olef}^{cod}); 4.27 (m, H_{olef}^{cod}), 3.35 (m, H_{olef}^{cod}).

Preparation of RuClH(cod)(PPFA) 3 and $Ru(\eta^3\text{-}C_8H_{13})$Cl-(PPFA) 4. Under analogous conditions to that described for **1**, with PPFA compound **4** was obtained as an orange-red oil which was triturated with hexane to yield **4** as a brown solid. Amounts are as follows: RuClH(bpzm)(cod): 70.9 mg, 0.18 mmol; PPFA: 80.0 mg, 0.18 mmol. Yield: (51.9 mg, 42%). Found: C, 59.5; H, 5.9 ; N, 2.1. $C_{34}H_{41}$ClNPFeRu requires C, 59.4; H, 6.0; N, 2.0%. IR: ν_{max}/cm^{-1} 230 (Ru–Cl). ^{1}H-NMR (benzene-d_6): δ 1.14 (d, J_{HH} = 6.8, Me); cyclooctenyl group: (numbering according to Fig. 2): 4.34 (1H, m, H_1); 3.36 (1H, m, H_2); 2.45 (1H, m, H_{8A}); 2.05 (1H, dt, H_{6B}) 1.7–1.9 (2H, m, H_3 and H_{4B}); 1.55 (1H, m, H_{7B}); 1.25–1.45 (2H, m, H_{5A} and H_{7A}); 1.23 (1H, m, H_{5B}); 1.05 (1H, dt, H_{6A}); 0.65 (1H, m, H_{4A}); -0.55 (1H, m, H_{8B}). ^{13}C{^{1}H}-NMR (benzene-d_6): δ 59.32 (s, C_1); 81.26 (s, C_2); 46.09 (s, C_3); 33.12, 30.23, 27.79, 23.20 (s, $C_{4\text{-}7}$); 28.75 (d, J_{CP} = 4.5, C_8), 9.47 (s, Me). After a reaction time of only 1 h, compound **3** was obtained as a mixture with **4**, but in solution **3** is irreversibly transformed into **4**.

Preparation of $RuCl_2(PPh_3)$(PTFA) 5. A degassed solution of 163 mg of $RuCl_2(PPh_3)_3$ (0.17 mmol) and 80 mg of PTFA (0.17 mmol) in 5 mL of toluene was stirred for 1.5 h. The resulting green solution was evaporated to dryness and a gummy residue was obtained. The product was purified by chromatography on Silica 60 (25 × 1 cm). First, free PPh_3 was removed by elution with toluene, then the product was eluted with THF. This solution was evaporated to dryness and the resulting oil was washed and triturated with hexane giving **5** as a green solid. Yield: 122.6 mg (0.14 mmol, 80%). Found: C, 61.4; H, 4.9 ; N, 1.5. $C_{46}H_{45}Cl_2NP_2FeRu$ requires C, 61.3; H, 5.0; N, 1.6%. IR: ν_{max}/cm^{-1} 322 (Ru–Cl). ^{1}H-NMR (chloroform-*d*), homoannular chain: δ 2.81, m; 2.42, dd; 2.31, t (2H); 2.22, t; 2.10, m. ^{13}C{^{1}H}-NMR (chloroform-*d*), homoannular chain: δ 24.20, s; 22.94, s; 21.98, s.

Preparation of $RuH(\eta^2\text{-}BH_4)(PPh_3)$(PTFA) 6. A degassed solution of 30.0 mg of **5** (0.033 mmol) and 17.8 mg of KBH_4 (0.33 mmol) in 5 mL of dry ethanol was stirred for 2.5 h. After evaporation to dryness the residue was washed with toluene (20 mL). The resulting solution was filtered and evaporated to dryness. Complex **6** was obtained as a yellow solid. Yield: (16.8 mg, 60%). Found: C, 65.0; H, 5.9 ; N, 1.7. $C_{46}H_{50}BNP_2FeRu$ requires C, 65.3; H, 6.0; N, 1.7%. IR: ν_{max}/cm^{-1} 2042 (Ru–H), 2371 and 2300 (BH_t), and 1914 and 1900 (μ-Ru–H–B). ^{1}H-NMR (benzene-d_6, −70 °C), **6M**: δ −4.40 (1H, bs, μ-Ru–H_{b1}–B), −6.60 (1H, d, J_{HP} = 40.8, μ-Ru–H_{b2}–B), 4.82 (1H, bs, terminal BH_2), 4.50 (1H, bs, terminal BH_2); **6m**: −3.54 (1H, bs, μ-Ru–H_{b1}–B), -6.35 (1H, d, μ-Ru–H_{b2}–B); 9.06 (2H, m, *ortho* Ph_{down}, −70 °C). ^{13}C{^{1}H}-NMR (benzene-d_6), homoannular chain: **6M**: δ 23.78 (s); 23.10 (s); 22.46 (s).

X-Ray data collection, structure determination, and refinement of complexes 1 and 4

The crystallographic data and experimental details are given in Table 3. Crystals of **1** and **4** were grown from THF–pentane. The data collection was performed on a NONIUS-MACH3 diffractometer equipped with a graphite monochromator and Mo-Kα radiation (λ = 0.71073 Å) using an $\omega/2\theta$ scan technique to a maximum value of θ = 28°. Data were corrected for Lorentz and polarisation effects and semi-empirical absorption correction was carried out on the basis of an azimuthal scan.[23]

The structures were solved using direct methods (SIR92)[24] and refined first isotropically by full-matrix least-squares using SHELXL-93[25] program and then anisotropically by blocked full-matrix least-squares for all the non-hydrogen atoms. The hydrogen atoms were included in calculated positions and refined "riding" on their parent carbon atoms, except the hydrogen atoms in the cyclooctenyl ligand of **4** and the hydride of **1**. Despite the proximity to the heavy ruthenium nuclei, the hydride position in **1** could be calculated in the difference Fourier map and refined isotropically.

CCDC reference number 186/1678.

See http://www.rsc.org/suppdata/dt/1999/4031/ for crystallographic files in .cif format.

Acknowledgements

We gratefully acknowledge the Dirección General de Investigación Científica y Técnica (DGICYT, Grant PB95-0901 and Acción Integrada project HU96-0020, Ciudad Real, Spain),

the Fonds zur Förderung der Wissenschaftlichen Forschung (Project P09859-CHE) and Österreichischer Akademischer Austauschdienst (ÖAD, Acción Integrada project 28/97, Wien, Austria).

References

1 T. Hayashi, in *Ferrocenes, Homogeneous Catalysis, Organic Synthesis and Materials Science*, ed. A. Togni and T. Hayashi, VCH, Weinheim, 1995, pp. 105.
2 A. Togni, *Angew. Chem.*, *Int. Ed.*,1996, **35**, 1475.
3 (*a*) *Catalytic Asymmetric Synthesis*, ed. I. Ojima, VCH, Weinheim, 1993; (*b*) R. Noyori, in *Asymmetric Catalysis in Organic Synthesis*, John Wiley & Sons, New York, 1994.
4 G. E. Rodgers, W. R. Cullen and B. R. James, *Can. J. Chem.*, 1983, 1314.
5 N. C. Zanetti, F. Spindler, J. Spencer, A. Togni and G. Rihs, *Organometallics*, 1996, **15**, 860.
6 (*a*) B. Jedlicka, M. Widhalm and W. Weissensteiner, *J. Chem. Soc., Chem. Commun.*, 1993, 1329; (*b*) H. Wally, K. Schlögl, W. Weissensteiner and M. Widhalm, *Tetrahedron: Asymm.*, 1993, **4**, 285; (*c*) H. Wally, C. Kratky, W. Weissensteiner, M. Widhalm and K. Schlögl, *J. Organomet. Chem.*, 1993, **450**, 185; (*d*) A. Mernyi, C. Kratky, W. Weissensteiner and M. Widhalm, *J. Organomet. Chem.*, 1996, **508**, 209; (*e*) G. Kutschera, C. Kratky, W. Weissensteiner and M. Widhalm, *J. Organomet. Chem.*, 1996, **508**, 195; (*f*) B. Jedlicka, R. E. Rülke, W. Weissensteiner, R. Fernández-Galán, F. A. Jalón, B. R. Manzano, J. Rodríguez-de la Fuente, N. Veldman, H. Kooijman and A. L. Spek, *J. Organomet. Chem.*, 1996, **516**, 97; (*g*) H. Wally, U. Nettekoven, W. Weissensteiner, A. Werner and M. Widhalm, *Enantiomer*, 1998, **2**, 441; (*h*) F. Gómez-de la Torre, F. A. Jalón, A. López-Agenjo, B. R. Manzano, A. Rodríguez, T. Sturm, W. Weissensteiner and M. Martínez-Ripoll, *Organometallics*, 1998, **17**, 4634.
7 M. Fajardo, A. de la Hoz, E. Diéz-Barra, F. A. Jalón, A. Otero, A. Rodríguez, J. Tejeda, D. Belletti, M. Lafranchi and M. A. Pellinghelli, *J. Chem. Soc., Dalton Trans.*, 1993, 1935.
8 (*a*) J. M. Williams, R. K. Brown, A. J. Schultz, G. D. Stucky and S. D. Ittel, *J. Am. Chem. Soc.*, 1978, **100**, 7407; (*b*) R. L. Harlow, R. J. McKinney and S. D. Ittel, *J. Am. Chem. Soc.*, 1979, **101**, 7496; (*c*) R. K. Brown, J. M. Williams, A. J. Schultz, G. D. Stucky, S. D. Ittel and R. L. Harlow, *J. Am. Chem. Soc.*, 1980, **102**, 981; (*d*) T. V. Ashworth, D. C. Liles and E. Singleton, *Organometallics*, 1984, **3**, 1851.
9 See, for example, (*a*) P. A. Chaloner, M. A. Esteruelas, F. Joó and L. A. Oro, in *Homogeneous Hydrogenation*, Kluwer Academic Publishers, Dordrecht, 1994; (*b*) M. A. Esteruelas, M. P. García, A. M. López, L. A. Oro, N. Ruiz, C. Schlünken, C. Valero and H. Werner, *Inorg. Chem.*, 1992, **31**, 5580; (*c*) M. A. Esteruelas and L. A. Oro, *Chem. Rev.*, 1998, **98**, 577 and references therein.
10 (*a*) C. Potvin, J. M. Manoli, G. Pannetier and R. Chevalier, *J. Organomet.Chem.*, 1978, **146**, 57; (*b*) C. Potvin, J. M. Manoli, G. Pannetier and N. Platzer, *J. Organomet. Chem.*, 1981, **219**, 115; (*c*) B. Delavaux, B. Chaudret, J. Devillers, F. Dahan, G. Commenges and R. Poilblanc, *J. Am. Chem. Soc.*, 1986, **108**, 3703; (*d*) A. Romero, A. Vegas, A. Santos and A. M. Cuadro, *J. Chem. Soc., Dalton Trans.*, 1987, 183; (*e*) T. Yoshida, T. Adachi, T. Ueda, F. Goto, K. Baba and T. Tanaka, *J. Organomet. Chem.*, 1994, **473**, 225.
11 R. Férnandez-Galán, F. A. Jalón, B. R. Manzano, J. Rodríguez-de la Fuente, M. Vrahami, B. Jedlicka, W. Weissensteiner and G. Jogl, *Organometallics*, 1997, **16**, 3758.
12 R. Dorta and A. Togni, *Organometallics*, 1998, **17**, 3423.
13 (*a*) M. Brookhart and M. L. H. Green, in *Progress in Inorganic Chemistry*, ed. S. J. Lippard, Wiley Interscience, New York, 1988, Vol. 36, pp. 1; (*b*) R. H. Crabtree, *Angew. Chem.*, *Int. Ed. Engl.*, 1993, **32**, 789.
14 (*a*) M. Bortolin, U. E. Bucher, H. Rüegger, L. M. Venanzi, A. Albinati, F. Lianza and S. Trofimenko, *Organometallics*, 1992, **11**, 2514; (*b*) A. Albinati, F. Lianza, P. Pregosin and B. Müller, *Inorg. Chem.*, 1994, **33**, 2522.
15 (*a*) C. R. S. M. Hampton, I. R. Butler, W. R. Cullen, B. R. James, J. P. Charland and J. Simpson, *Inorg. Chem.*, 1992, **31**, 5509; (*b*) P. R. Hoffman and K. G. Caulton, *J. Am. Chem. Soc.*, 1975, **97**, 4221.
16 (*a*) M. W. Schoonover, C. P. Kubiak and R. Eisenberg, *Inorg. Chem.*, 1978, **17**, 3050; (*b*) T. V. Ashworth, M. J. Nolte, R. H. Reimann and E. Singleton, *J. Chem. Soc., Chem. Commun.*, 1977, 757.
17 M. S. Lupin and B. L. Shaw, *J. Chem. Soc. A*, 1968, 741.
18 (*a*) R. H. Crabtree and A. J. Pearman, *J. Organomet. Chem.*, 1978, **157**, 335; (*b*) D. G. Holah, A. N. Hughes and B. C. Hui, *Can. J. Chem.*, 1976, **54**, 320; (*c*) H. Suzuki, D. H. Lee, N. Oshima and Y. Moro-oka, *Organometallics*, 1987, **6**, 1569; (*d*) J. A. Statler, G. Wilkinson, M. Thornton-Pett and M. B. Hursthouse, *J. Chem. Soc., Dalton Trans.*, 1984, 1731; (*e*) H. Werner, M. A. Esteruelas, E. Sola and L. A. Oro, *J. Organomet. Chem.*, 1987, **120**, 11.
19 J. B. Letts, T. J. Mazanec and D. W. Meek, *J. Am. Chem. Soc.*, 1982, **104**, 3898.
20 I. Demachy, M. A. Esteruelas, Y. Jean, A. Lledós, F. Maseras, L. A. Oro, C. Valero and F. Volatron, *J. Am. Chem. Soc.*, 1996, **118**, 8388.
21 P. S. Hallman, T. A. Stephenson and G. Wilkinson, *Inorg. Synth.*, 1970, **12**, 237.
22 T. Hayashi, T. Mise, M. Fukushima, M. Kagotani, N. Nagashima, Y. Hamada, A. Matsumoto, S. Kawakami, M. Konishi, K. Yamamoto and M. Kumada, *Bull. Chem. Soc. Jpn.*, 1980, **53**, 1138.
23 A. C. T. North, D. C. Phillips and F. S. Mathews, *Acta Crystallogr., Sect. A*, 1968, **24**, 351.
24 A. Altomare, G. Cascarano, C. Giacovazzo, A. Guagliardi, M. C. Burla, G. Polidori and M. Camalli, *J. Appl. Cryst.*, 1994, 435.
25 G. M. Sheldrick, SHELXL93, Program for the Refinement of Crystal Structures from diffraction data, University of Göttingen, 1993.

Paper 9/04832D